Significance of Heterochronic Differences in Neural Crest Cell Migration and Sclerotomal Development in Evolution of the Trunk Body Organization from Agnathans to Gnathostomes

Masashi Hirata*, Kazuo Ito and Kazuhiko Tsuneki

Department of Biology, Graduate School of Science, Osaka University, 1-16 Machikaneyama, Toyonaka, Osaka 560-0043, Japan

ABSTRACT—The process of neural crest cell migration differs between the lamprey and swordtail [Hirata *et al.*, Zoological Science 14: 305-312 (1997)]. In swordtail embryos, neural crest cells in the ventral pathway are distributed ventrally beyond the notochord at all axial levels of the trunk. In contrast, no neural crest cells are seen ventrally beyond the notochord in post-branchial regions of lamprey embryos, although in the branchial regions some cells migrate ventrally beyond the notochord. Since sclerotomal development is essential in the formation of ventral pathways in avian and mammalian embryos, sclerotomal development in lamprey and swordtail embryos was examined to understand the mechanism underlying the differences in neural crest cell migration between these two animals. Sclerotomal development and neural crest cell migration progressed concurrently in the swordtail trunk. In the lamprey, the formation of the sclerotome was regionally different along the antero-posterior axis. In the branchial region, where neural crest cells are observed ventrally beyond the notochord, sclerotomal development was closely correlated with neural crest cell migration as in the swordtail. The overt sclerotome was not observed in the lamprey trunk posterior to the branchial region during the period of neural crest cell migration. These observations suggest that differences in the timing of neural crest cell migration and sclerotomal development generate the differences in migration of lamprey and swordtail neural crest cells along the ventral pathways. Heterochronic differences in sclerotomal development correlated with neural crest cell migration may have some significance in the evolution of the trunk body organization from agnathans to gnathostomes.

INTRODUCTION

The vertebrates may be divided into two groups; the agnathans and the gnathostomes. Living agnathans have a long, slender, eel-like body shape and consist of two subgroups, the hagfish and the lamprey. The body organization of gnathostomes and agnathans differs in two major ways. Neither hagfish nor lamprey possess a jaw in the head or sympathetic nerve chains in the trunk (Fig. 1; Nicol, 1952; Burnstock, 1969; Healey, 1972). Bone and cartilage in the jaw and the sympathetic nerve chain are all derived from embryonic neural crest cells, which emerge from the dorsal region of the neural tube and migrate extensively through the embryo (Le Douarin, 1982; Hall and Hörstadius, 1988). Thus, changes in neural crest development may account for the differences in body organization between gnathostomes and agnathans.

Our previous study showed that a certain population of neural crest cells of both the brook lamprey and the viviparous teleost, the swordtail, is immunoreactive to the HNK-1 monoclonal antibody (Hirata *et al.*, 1997), which has been extensively used for the detection of neural crest cells and their derivatives (Erickson *et al.*, 1989; Sadaghiani and Vielkind, 1989, 1990; Laudel and Lim, 1993; Hou and Takeuchi, 1994; Sadaghiani *et al.*, 1994). We also found that neural crest cell migration in the medial portions of the somites, that is the migration along the ventral pathways, differs between the lamprey and the swordtail (Hirata *et al.*, 1997). The formation of ventral pathways depends on sclerotomal development (Bronner-Fraser, 1986; Loring and Erickson, 1987; Teillet *et al.*, 1987; Erickson *et al.*, 1989) and neural crest cells migrating along ventral pathways participate in the formation of the sympathetic nerve chain (Le Douarin, 1982). Thus, it is conceivable that differences in neural crest cell migration correlated with sclerotomal development generate the difference in lamprey and swordtail trunk body organization. Therefore, we examined neural crest cell migration along the ventral pathways during development of the sclerotome in lamprey and swordtail embryos.

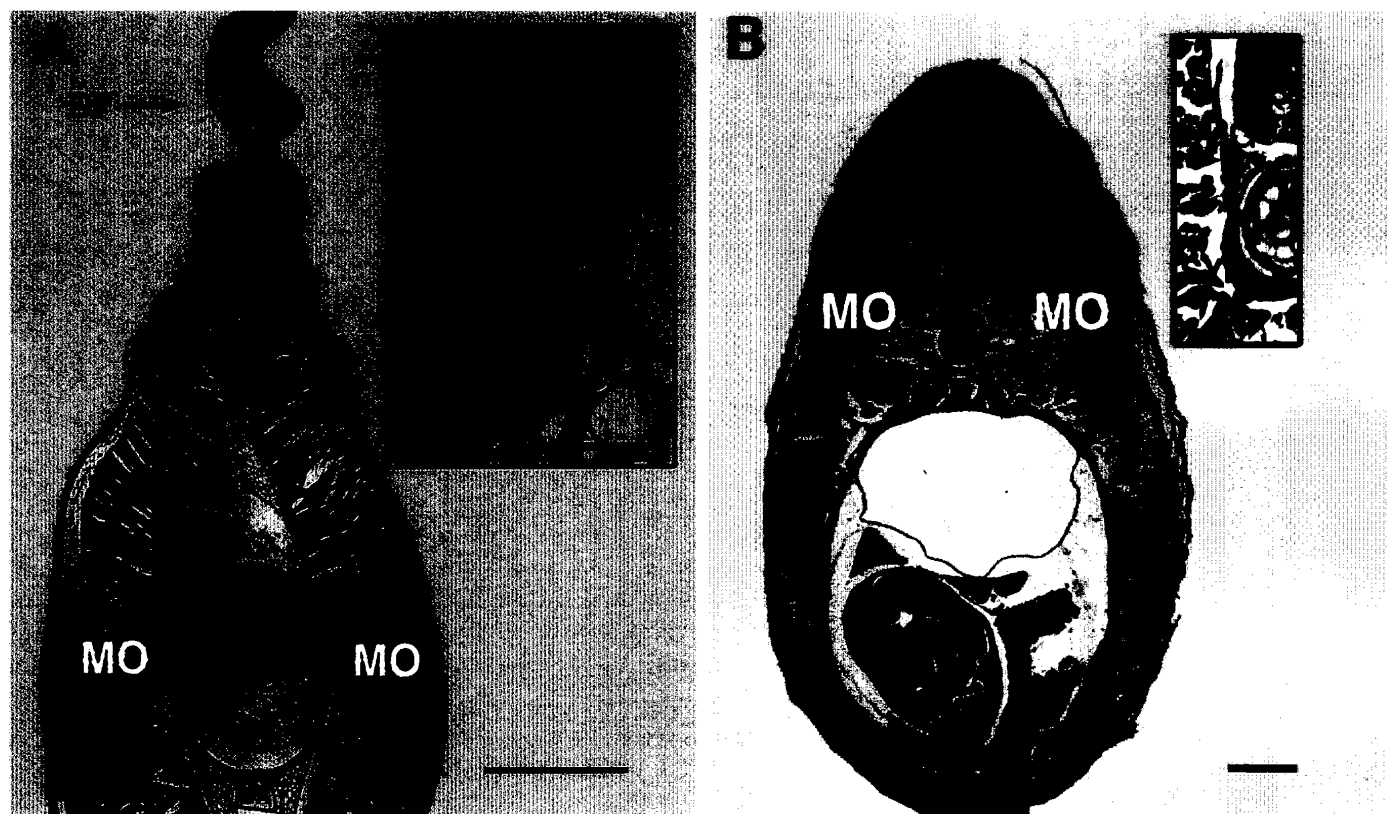* Corresponding author: Tel. +81-6-6850-5807;
 FAX. +81-6-6850-5817.

Fig. 1. Basic features of the adult lamprey and swordtail trunk. (**A**) Transverse section of the lamprey trunk. An arrowhead indicates the dorsal root ganglion. (**B**) Transverse section of the swordtail trunk. A sympathetic nerve chain (SYM) is present in the swordtail but not in the lamprey. DF, dorsal fin; DA, dorsal aorta; DRG, dorsal root ganglion; MO, myomere; NO, notochord; SC, spinal cord. Scale bars: **A**, 1 mm; **A** inset, 50 μm; **B**, 100 μm; **B** inset, 20 μm.

MATERIALS AND METHODS

Experimental animals

Embryos of the brook lamprey, *Lampetra reissneri*, and the swordtail, *Xiphophorus helleri*, were used. Sexually mature lampreys were kept in tank water at 20°C and embryos were obtained after natural spawning or artificial fertilization. Lamprey embryos were staged according to the criteria of Tahara (1988) and were used at stages 22-30. Swordtails were kept in an aquarium at 25°C and pregnant females were sacrificed at appropriate intervals. Their embryos were used at stages 8-23 (Tavolga, 1949). The numbers of somites at the various developmental stages of the swordtail and lamprey embryos examined in this study are listed in Table 1.

Histology

Embryos were fixed with Bouin's fixative. After dehydration in an ethanol-toluene series, they were embedded in Paraplast (Oxford Labware, St. Louis, MO, USA). Transverse sections were serially cut at a thickness of 6 to 10 μm. Sections were pre-stained with alcian blue (pH 2.5) for 2 hr to visualize the sclerotomal region and post-stained by Masson-Goldner's method or hematoxylin and eosin. They were mounted with Entellan (Merck, Darmstadt, Germany).

Immunohistochemistry

Embryos were fixed overnight in a 4% solution of paraformaldehyde in phosphate-buffered saline (PBS, pH 7.4) at 4°C and then washed several times with PBS. The fixed embryos were immersed in 10% to 30% sucrose in PBS and embedded in OCT compound (Miles, Elkhart, IN, USA). Serial 10−15-μm sections were attached to albumin-coated glass slides. Immunohistochemistry was performed according to methods described previously (Hirata *et al.*, 1997). The following primary antibodies were used: (1) HNK-1 (Becton Dickinson, San Jose, CA, USA; Lot 40557), (2) mouse monoclonal antibody against native chondroitin sulfate, CS-56 (Seikagaku Corp., Tokyo), (3) rabbit antiserum to human fibronectin (anti-FN; Cappel, Durham, NC, USA) for the identification of swordtail fibronectin, and (4) rabbit

Table 1. Somite number in developmental stages of lamprey and swordtail embryos

swordtail		lamprey	
developmental stage[¶]	somite number	developmental stage[¶¶¶]	somite number
Stage 8-11	≦20	Stage 22	18-19
Stage 12	21	Stage 23	28
Stage 13	22	Stage 24	40-43
Stage 14	24	Stage 25	60
Stage 15	25	Stage 27	80
Stage 16-23	26	Stage 30	85≦

[¶] According to Tavolga (1949).
[¶¶¶] According to Tahara (1988).

polyclonal antibody against human fibronectin (anti -FN; Calbiochem, Sandiego, CA, USA) which identifies lamprey fibronectin (Wright, 1986). The following affinity-purified secondary antibodies were used: (1) FITC-conjugated goat anti-mouse immunoglobulins (IgG, IgA, IgM) (Cappel), (2) rhodamine-conjugated goat anti-mouse immunoglobulins (Cappel), and (3) FITC-conjugated goat anti-rabbit IgG (Cappel). Double-stainings were performed with HNK-1 and anti-FN. HNK-1 staining always preceded that of anti-FN. Antibodies were used at the following dilutions: HNK-1, 1:40; CS-56, 1:500; anti-FN, 1:500; and secondary antibodies, 1:40. Primary antibodies except for CS-56 were applied to frozen sections overnight at 4°C. CS-56 was applied for 30 min at room temperature. In order to confirm that CS-56-positive materials were chondroitin sulfate, sections were treated with 0.1 U/ml protease free chondroitinase ABC (Seikagaku Corp.), which digests chondroitin sulfate chains specifically, for 3 hr at 37°C in a moist chamber (Nishikawa and Sasaki, 1993). Secondary antibodies were used for 1 hr at room temperature. Some sections of lamprey embryos were nuclear-stained with a 0.4 µg/ml solution of DAPI (4',6-diamino-2-phenylindole; Sigma, St. Louis, MO, USA) in PBS to make cell identification easier.

Estimation of volume of the somite and sclerotome

The length of somitic (myomere + sclerotome) and sclerotomal regions was measured along the dorso-ventral (D-V), proximo-distal (P-D) and antero-posterior (A-P) axes. The A-P length was estimated based on the number of serial transverse sections (each 10 µm thick) covering one somite or one sclerotome. The maximal D-V and P-D length were measured in these transverse sections by using an ocular micrometer. Since the somite and sclerotome are roughly regarded as being cubic, the volume of these structures was calculated as the multiplication of D-V, P-D and A-P values and the proportion of the sclerotome per somite was determined.

RESULTS

Relationship between sclerotomal development and neural crest cell migration in the swordtail

Fibronectin and chondroitin sulfate synthesized by sclerotomal cells play important roles in the formation of neural crest cell migratory routes in amniotes (Le Douarin, 1982). Therefore, we have examined temporal changes of the distribution of these extracellular matrix molecules in the sclerotome during the period of neural crest cell migration in the swordtail. In the premigratory stages of neural crest cells (Fig. 2A-D), morphologically detectable sclerotome was observed in the ventro-medial portion of the somite (Fig. 2D). The area surrounding the notochord, that contains the sclerotome, was CS-56-immunoreactive. Intense staining was seen in the boundary between the neural tube and the notochord (Fig. 2C). No fibronectin-like immunoreactivity was detected (Fig. 2B). In early migratory stages (Fig. 2E-H), HNK-1-positive cells (Fig. 2E) were present in the sclerotome that spread dorsally and reached the level of the neural tube (Fig. 2H). This observation shows that the ventral pathway is formed in the sclerotome, as in amniotes. The sclerotome contained FN and CS-56-positive materials (Fig. 2F, G). In intermediate-late migratory stages (Fig. 2I-L), the sclerotome reached the dorsal-most level of the neural tube (Fig. 2L) and contained HNK-1-positive cells (Fig. 2I). FN and CS-56-positive materials were observed in the sclerotome (Fig. 2J, K). CS-56-positive materials disappeared in sections treated with chondroitinase ABC

(data not shown). These results indicate that the swordtail sclerotome contains FN and CS-56-positive chondroitin sulfate (CS), and that their expression in the sclerotome is correlated with HNK-1-positive neural crest cell migration along the ventral pathway. Furthermore, sclerotomal development along the antero-posterior axis progressed concomitantly with neural crest cell migration (Fig. 3). HNK-1-immunoreactive cells in the ventral pathway were observed ventrally beyond the notochord throughout the swordtail trunk.

Regional differences in neural crest cell distribution in the lamprey trunk

HNK-1-positive neural crest cells appeared in the lamprey trunk at stage 23 (Hirata et al., 1997). The distribution of these cells in the ventral pathway shifted caudally from stage 23 to stage 27. There were regional differences in the distribution of HNK-1-immunoreactive cells in the trunk. In the branchial region, the distribution of the cells in the ventral pathway expanded ventrally beyond the notochord (Fig. 4A). Careful observations of serial transverse sections indicated that HNK-1-positive cells at the notochord level in this region are distributed at intervals of about 60 µm which corresponds to the length of one somite along antero-posterior axis. This means that their distribution in the ventral pathway is restricted to the intersomitic space at the notochord level. In the post-branchial trunk, no HNK-1-positive cells were observed ventrally beyond the boundary between the neural tube and notochord (Fig. 4B). These regional differences along the antero-posterior axis are compatible with the observation of the distribution of melanophores which are a typical derivative of neural crest cells even in the lamprey (Newth, 1956). We observed melanophores in the area surrounding the notochord in the branchial region (data not shown) but not in the space between the notochord and somite in the post-branchial region (Hirata et al., 1997).

Relationship between sclerotomal development and neural crest cell migration in the lamprey

Since sclerotomal development in the swordtail is closely correlated with neural crest cell migration along the ventral pathway, we have explored their correlation in the lamprey. In the branchial region where HNK-1-positive cells are distributed ventrally beyond the notochord, cell masses associated with CS-56-positive materials were observed at the boundary between the neural tube and notochord and near the ventro-lateral sides of the notochord (Fig. 5A-D). These cell masses appeared intersegmentally (Fig. 5E). This intersegmental distribution was similar to that of HNK-1-positive cells at the notochord level in the ventral pathway (Fig. 4A). Since CS-56 immunoreactivity disappeared after digestion with chondroitinase ABC (data not shown), CS-56-positive materials represented lamprey CS. The CS-containing region extended caudally up to the 20-somite level with advancing developmental stages (Fig. 7), but CS-containing regions were not found in the post-branchial trunk posterior to the 20-somite level during the period in which HNK-1-positive cells were
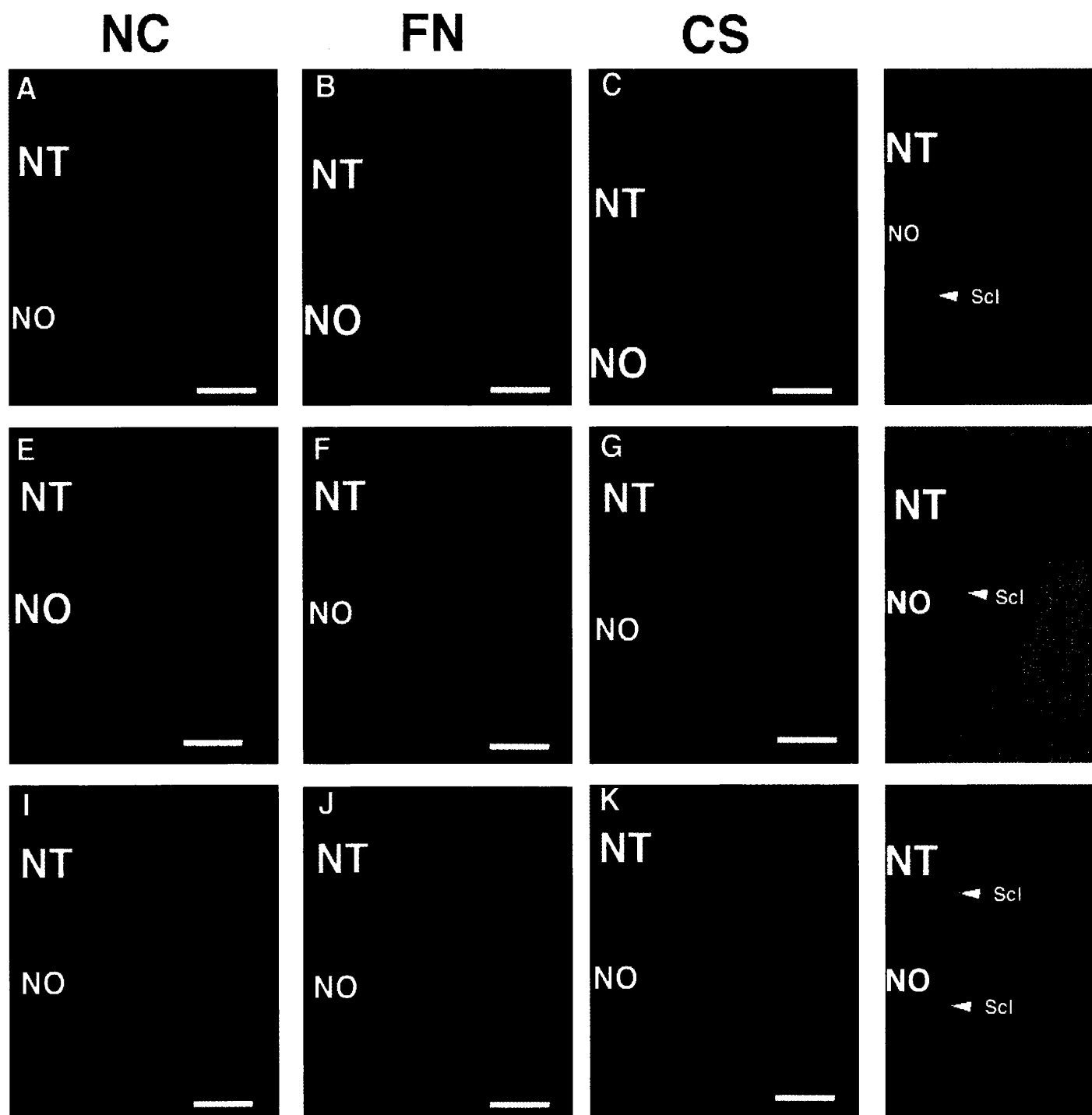
NC   FN   CS

Fig. 2. Sclerotomal development during neural crest cell migration in swordtail embryos. (**A-D**) Premigratory stages of neural crest cells in the ventral pathway. Transverse sections at 21-somite levels of stage 13 embryos. (**E-H**) Early migratory stages. Transverse sections at 17-somite levels of stage 12 embryos. (**I-L**) Intermediate-late migratory stages. Transverse sections at 10-somite levels of stage 12 embryos. Sections were stained with HNK-1 (**A, E, I**), antifibronectin (**B, F, J**) and CS-56 (**C, G, K**). **D, H** and **L** show sections stained histologically. The distribution of neural crest cells (NC) and fibronectin (FN) was examined in sections double-stained with HNK-1 and anti-fibronectin. NO, notochord; NT, neural tube; Scl, sclerotome. Scale bars: 20 μm.

present in the ventral pathway (Fig. 5F-H; Fig. 7). In the branchial region, loose mesenchymal cells were histologically observed in similar portions to the CS-containing regions (Fig. 6A). No mesenchymal cells were found beside the notochord in the post-branchial region (Fig. 6B). Moreover, cartilage, a main derivative of the sclerotome, was formed in the branchial region almost corresponding to the CS-containing region after stage 30 (Fig. 6C). No cartilage was observed in

the post-branchial trunk during the developmental stages examined (Fig. 6D). These observations strongly suggest that the CS-containing region located intersegmentally in the branchial region is the lamprey sclerotome. In *Lampetra fluviatilis* embryos, Damas (1944) histologically found the sclerotome in a region corresponding to the CS-containing region detected in the present observation. Taken together, these results suggest that in lamprey embryos, sclerotomal development
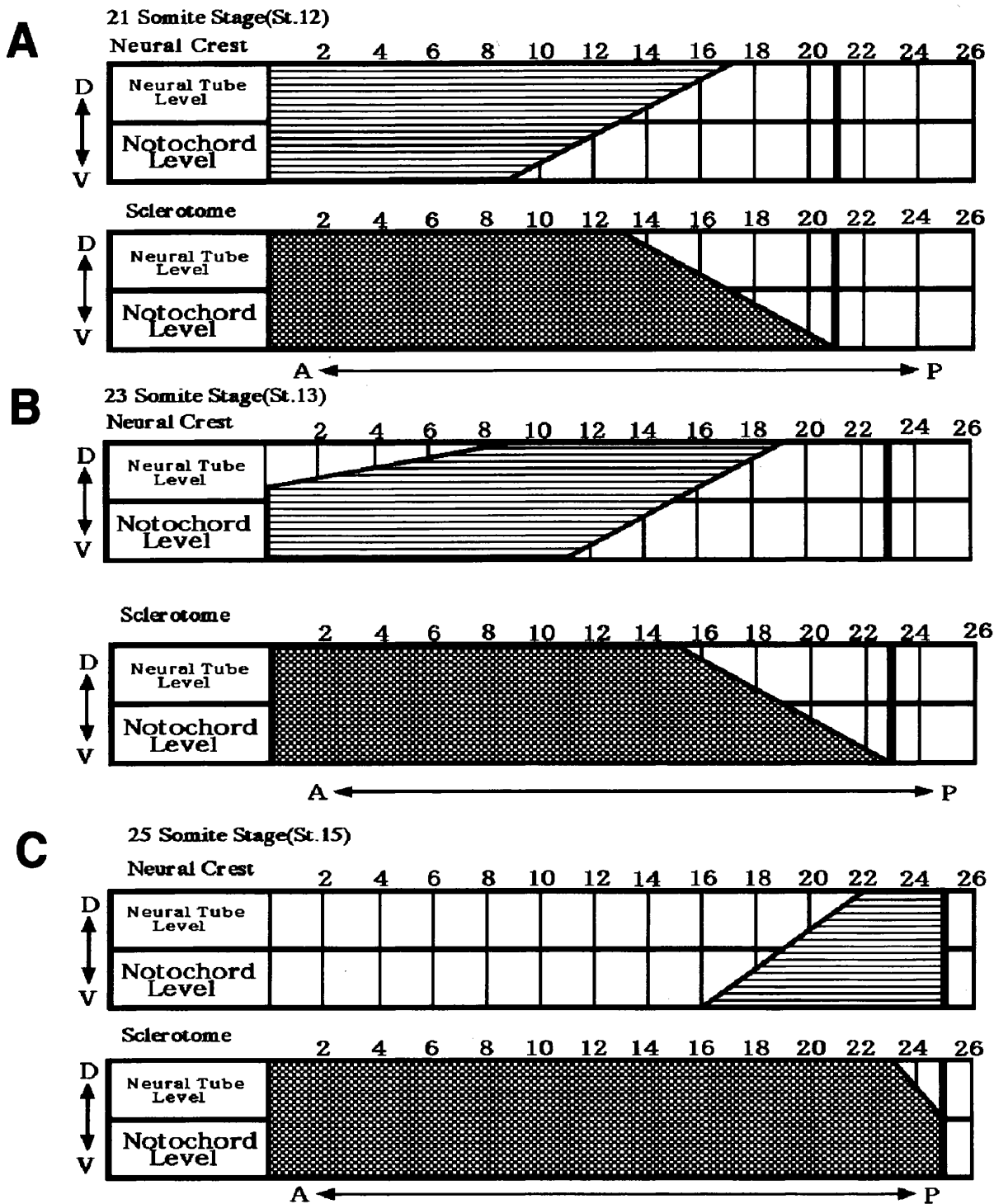
Fig. 3. Spatial and temporal changes in sclerotome formation during neural crest cell migration along the ventral pathway in swordtail embryos. Striped area displays somitic levels where neural crest cells migrate along ventral pathways at stages 12 (**A**), 13 (**B**) and 15 (**C**). Hatched area represents somitic levels where the sclerotome is formed at the corresponding stages. Numerals show somite numbers. Thick vertical lines correspond to the last somitic levels at respective stages. A, anterior; P, posterior; D, dorsal; V, ventral.

progresses concurrently with the neural crest cell migration only in the branchial regions, and in the post-branchial regions neural crest cell migration occurs without overt development of the sclerotome (Fig. 7).

Volume of the sclerotome in lamprey and swordtail embryos

Since histological and immunohistochemical observations suggested that the size of the CS-containing sclerotomal region in the lamprey is much smaller than that in the swordtail, the volume of the sclerotome was measured in both embryos. Whereas the swordtail sclerotome occupied approximately 10% of the somite (sclerotome + myomere) at the respective somitic levels during the period in which HNK-1-positive neural crest cells were observed in the ventral pathway (Fig. 8), the proportion of the lamprey sclerotome was approximately 1% at somitic levels where the CS-containing region was observed (Fig. 8).
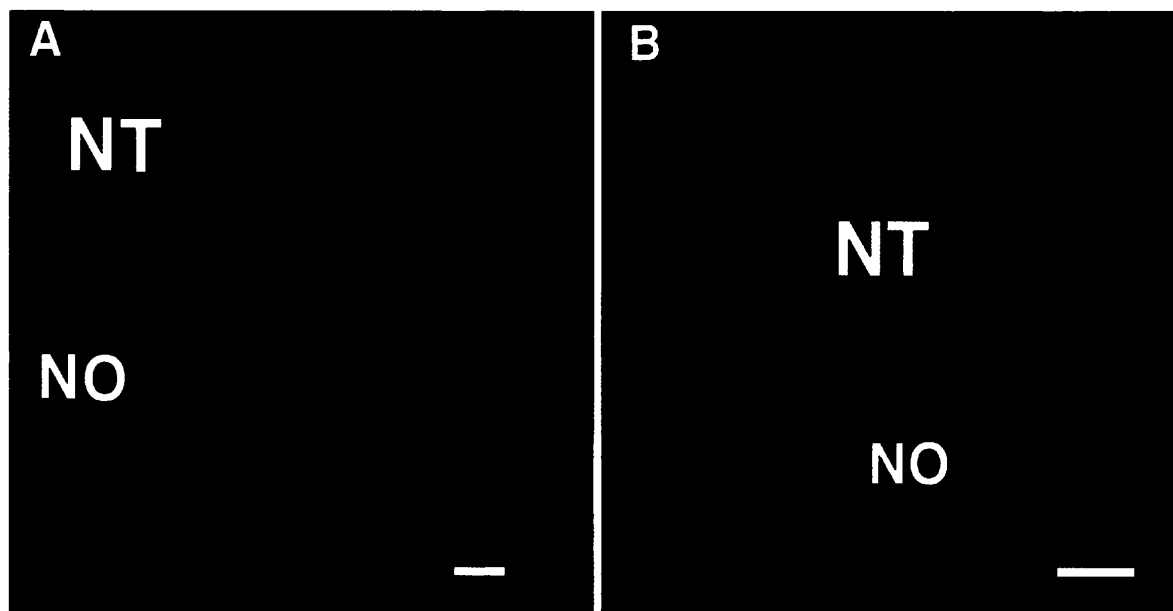
M. Hirata *et al.*

Fig. 4. Lamprey neural crest cells in the ventral pathway (red arrowheads). (**A**) Transverse section at 3-somite level in the branchial region of a stage 23 embryo. (**B**) Transverse section at 35-somite level in the post-branchial trunk of a stage 24 embryo. Sections were stained with HNK-1. NO, notochord; NT, neural tube. Scale bar: 20 μm.
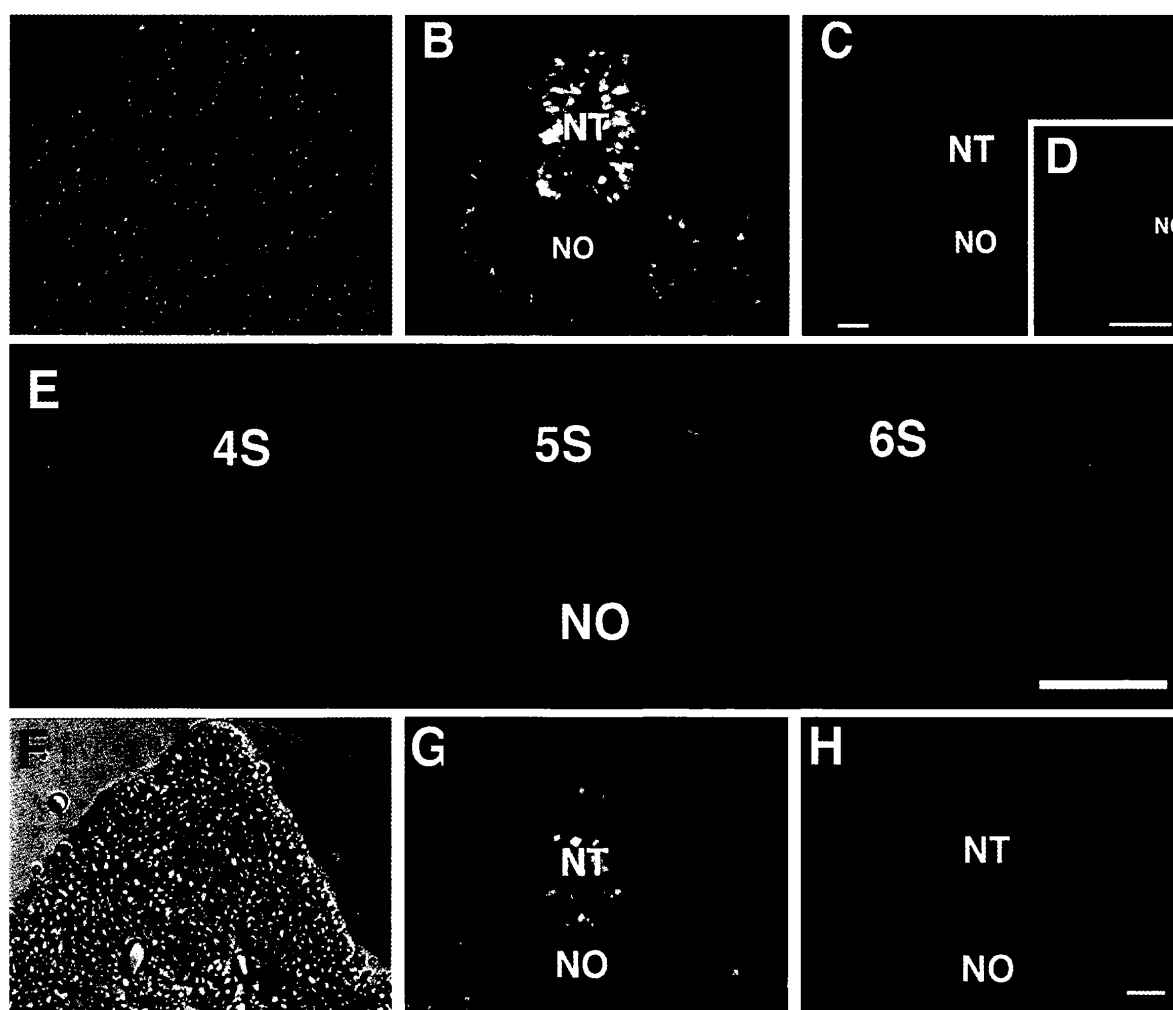

Fig. 5. CS-56-positive cell masses in the lamprey trunk. (**A-D**) Differential interference microscope image (**A**), nuclear staining (**B**) and fluorescence (**C**, **D**) micrograph of a transverse section at 6-somite level in the branchial region of stage 23 embryo. (**E**) Horizontal section at 4-6-somite levels (4S-6S) of a stage 23 embryo. Rostral is to the left. (**F-H**) Differential interference microscope image (**F**), nuclear staining (**G**) and fluorescence (**H**) micrograph of a transverse section at 30-somite level in the post-branchial region of stage 24 embryo. All sections were stained with antibody against native chondroitin sulfate, CS-56. NO, notochord; NT, neural tube. Scale bars: 20 μm.
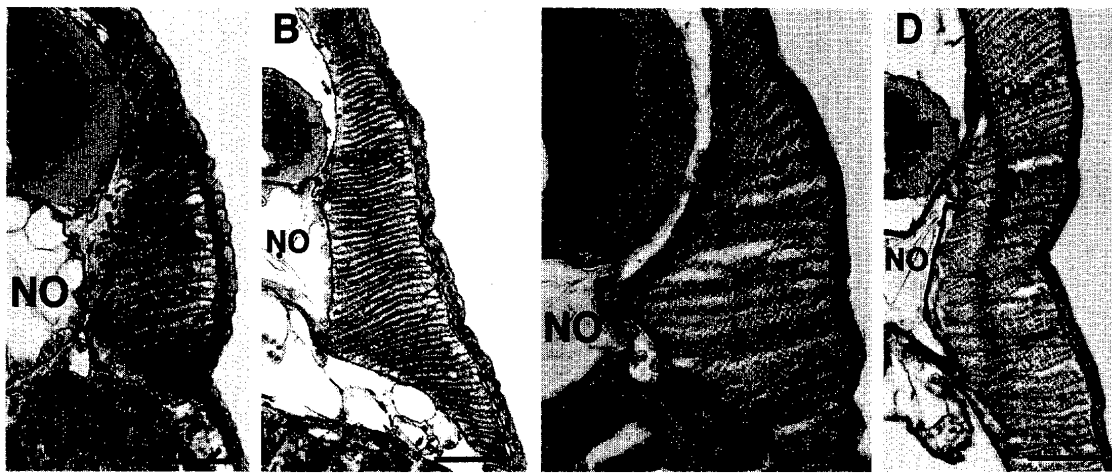
Fig. 6. (**A, B**) Histological sections of a stage 27 lamprey embryo. (**A**) Transverse section at 5-somite level in the branchial region. Mesenchymal cells (small arrowheads) are found in the space between the notochord and the myomere. (**B**) Transverse section at 30-somite level in the post-branchial region. (**C, D**) Histological sections of a stage 30 lamprey larva. (**C**) Transverse section at 5-somite level. Cartilage (large arrowhead) is observed beside the ventro-lateral portion of the notochord. (**D**) Transverse section at 30-somite level. The dorsal root ganglia (DRG), which are formed in the intersomitic space, are observed in all sections. NO, notochord; NT, neural tube. Scale bars: 50 μm.
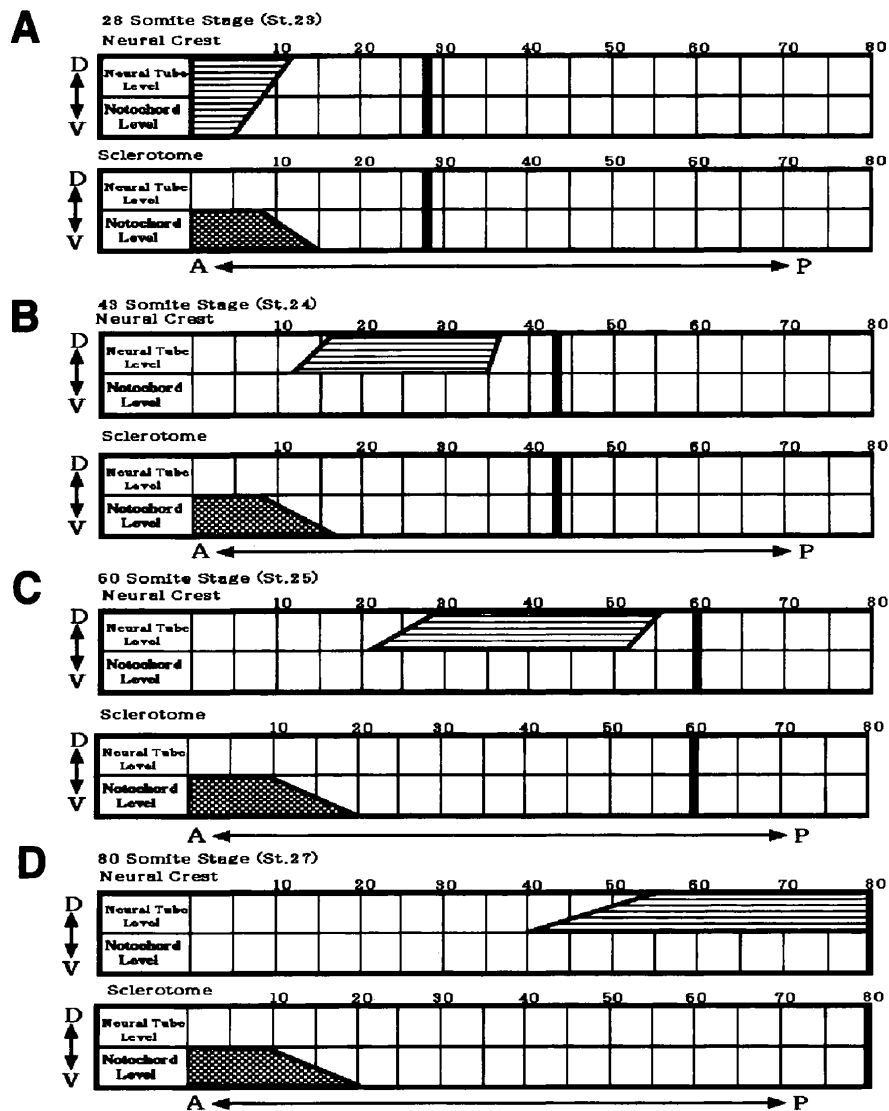

Fig. 7. Spatial and temporal changes of sclerotome formation during neural crest cell migration along the ventral pathway in lamprey embryos. Striped area displays somitic levels where neural crest cells migrate along the ventral pathway at stages 23 (**A**), 24 (**B**), 25 (**C**) and 27 (**D**). Hatched area represents somitic levels where the sclerotome is formed at the corresponding stages. Numerals show somite numbers. Vertical thick lines correspond to the last somitic levels at respective stages. A, anterior; P, posterior; D, dorsal; V, ventral.
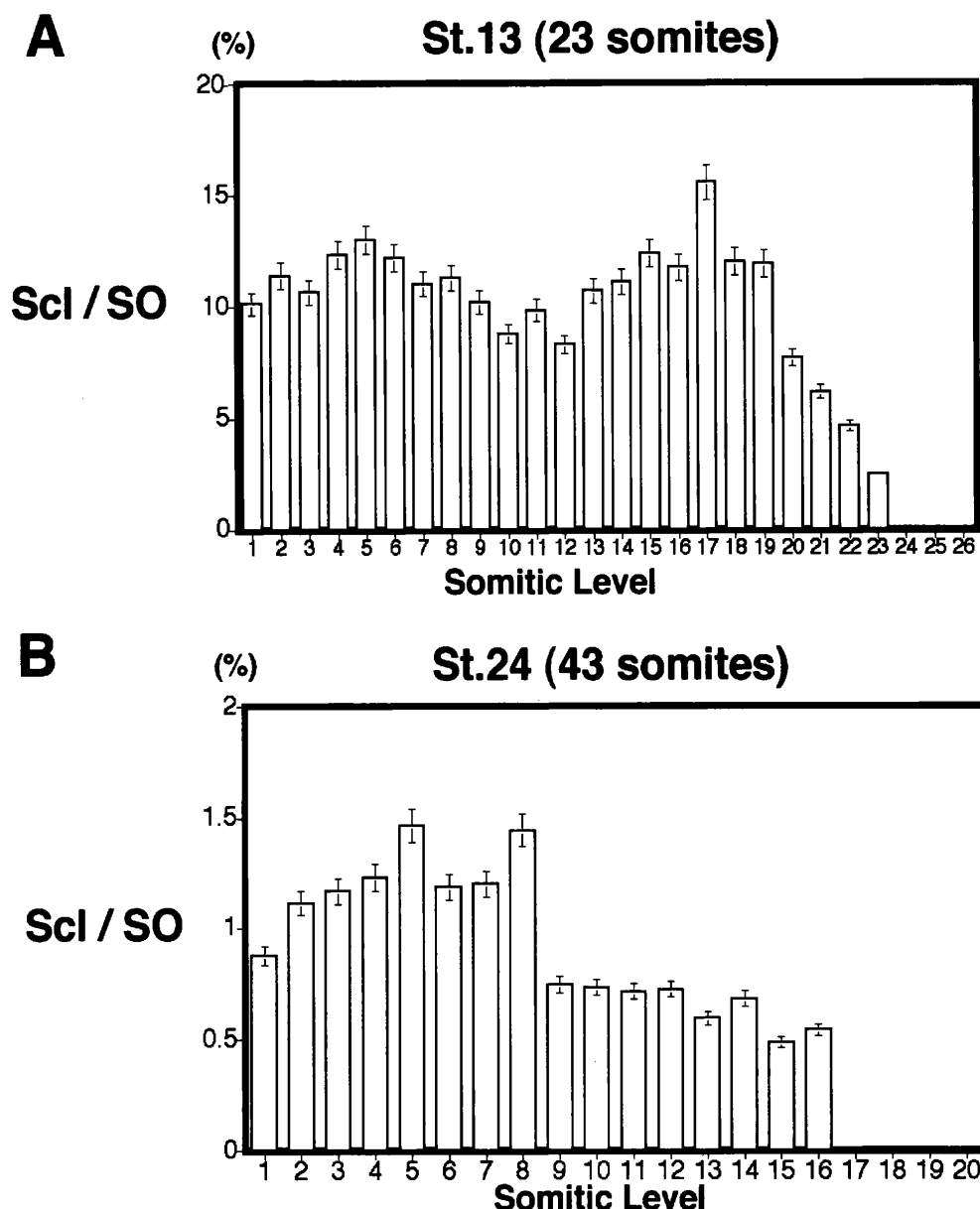
Fig. 8. Sclerotomal size at respective somitic levels during neural crest cell migration in stage (St.) 13 swordtail (**A**) and stage 24 lamprey (**B**) embryos. Percentage of the sclerotome per somite (Scl/SO) was calculated as described in Materials and Methods. It is noteworthy that the value of ordinate in **A** is 10-fold greater than that in **B**. The percentage was similar in stage 12, 13 and 15 swordtail embryos and in stage 23, 24 and 25 lamprey embryos.

DISCUSSION

In the present study, we have found clear differences in the patterns of neural crest cell distribution in ventral pathways between lamprey and swordtail embryos. Swordtail neural crest cells in the ventral pathway migrate ventrally beyond the notochord at all axial levels of the trunk. In swordtail embryos, sclerotomal development and neural crest cell distribution progress concurrently along both the antero-posterior and dorso-ventral axes throughout the trunk. Morin-Kensicki and Eisen (1997) have shown that zebrafish sclerotomal cells share a pathway with the migrating neural crest cells, and that the former migrate dorsally as the latter move ventrally. These results are consistent with our observations in the swordtail. The present data furthermore show that swordtail sclerotome contains CS and FN, supporting the observation

of Sadaghiani *et al.* (1994) who examined the distribution of extracellular matrix molecules in swordtail and platyfish embryogenesis. The subepidermal space also contains CS and FN (Fig. 2F, G, J, K). It is well known that other migratory pathways of trunk neural crest cells, so-called dorso-lateral pathways, are formed in this region (Le Douarin, 1982). Thus, these extracellular matrix molecules might contribute to the formation of the ventral pathway and dorso-lateral pathway in the swordtail.

While in the branchial region lamprey neural crest cells migrate ventrally beyond the notochord, no neural crest cells reach subnotochordal portions in the post-branchial region. In lamprey embryos, thus, the concomitant progression of sclerotomal development and neural crest cell migration occurs only in the branchial regions. Neural crest cells in these regions can translocate ventrally beyond the notochord in the

sclerotome located intersegmentally. The lamprey sclerotome is not found in the post-branchial region during the period of neural crest cell migration. Since there is cartilage that is possibly derived from the sclerotome in the post-branchial trunk of the adult lamprey (Hardisty, 1981), the progression of sclerotome formation along the antero-posterior axis may be much slower than that of neural crest cell migration in this animal. It is possible that coordination of the timing of neural crest cell migration and sclerotomal development is requisite for neural crest cells to migrate ventrally beyond the notochord.

HNK-1-positive cranial vagus ganglia are observed under the notochord in the branchial region (Hirata et al., 1997; Kuratani et al., 1997). Langille and Hall (1988), who extirpated pre-branchial and branchial neural crest cells in the sea lamprey (Petromyzon marinus), have shown that neural crest cells contribute to the branchial elements. It is conceivable that these components may originate from neural crest cells which have reached subnotochordal portions in the branchial region. Johnston (1908) reported the presence of nerve fibers and/or cells around the gut and blood vessels in the sea lamprey, and there are chromaffin cells in the heart and around the gut in the lamprey (Healey, 1972). However, it is not known whether there are preganglionic fibers from the spinal cord (Fritzsch and Northcutt, 1993). Thus, the chromaffin cells differ from distinct sympathetic nerve chains at the anatomical level (Nicol, 1952; Burnstock, 1969; Healey, 1972). Our previous study (Hirata et al., 1997) suggested that the chromaffin cells may be HNK-1-immunoreactive and derived from the branchial neural crest cells. This embryonic origin is similar to that of parasympathetic enteric neurons. Vagal visceral nerves are observed around the intestine (Healey, 1972), although it is unclear whether these nerves innervate the chromaffin cells. Detailed analyses of developmental processes of these cells may help clarify the evolutionary history of the autonomic nervous system.

The sympathoadrenal cell lineage is determined by specific transcription factors and their expression is controlled by distinct morphogenetic factors in mammalian and avian embryos (Anderson, 1993, 1997). These environmental factors are expressed at the same time and place as colonization of sympathoadrenal precursor crest cells (Reissmann et al., 1996; Shah et al., 1996). Valuable information about the evolutionary origin of the sympathetic nerve chain will be provided by the study of the presence or absence of these factors, the timing of their expression and their localization in lamprey and piscine embryos.

The anatomically distinct sympathetic nerve chain, which is a major derivative of neural crest cells migrating ventrally beyond the notochord in gnathostomes, is absent in the lamprey (Nicol, 1952; Burnstock, 1969; Healey, 1972). We propose the following as an underlying mechanism for the generation of the sympathetic nerve chain in gnathostomes. The timing of sclerotomal development and neural crest cell migration may have changed to progress concurrently in the overall trunk. This allowed neural crest cells to migrate ventrally beyond the notochord at all trunk levels and colonize the region where the appropriate environmental factors for formation of the sympathetic nerve chain are expressed. Thus, changes in the timing of sclerotomal development correlated with neural crest cell migration caused changes in sites of localization of neural crest cells. The interaction of these cells with the novel environment might have generated the sympathetic nerve chain. In addition, the sclerotomal size increased in gnathostomes and made it possible for a significant number of neural crest cells to migrate into the region where the sympathetic nerve chain is formed.

It is currently thought that changes in the timing of developmental events in evolutionary process (heterochronic changes) play important roles in evolution of the body organization (Gould, 1977; McKinney and McNamara, 1991; Richardson, 1995). This study may provide one example of these changes correlated with the formation of different body organization.

ACKNOWLEDGMENTS

REFERENCES

Anderson DJ (1993) Molecular control of cell fate in the neural crest: the sympathoadrenal lineage. Annu Rev Neurosci 16: 129–158

Anderson DJ (1997) Cellular and molecular biology of neural crest cell lineage determination. Trends Genet 13: 276–280

Bronner-Fraser M (1986) Analysis of the early stages of trunk neural crest migration in avian embryos using monoclonal antibody HNK-1. Dev Biol 115: 44–55

Burnstock G (1969) Evolution of the autonomic innervation of visceral and cardiovascular systems in vertebrates. Pharmacol Rev 21: 247–324

Damas H (1944) Recherches sur la développement de Lampetra fluviatilis L. Contribution à l'étude de la céphalogenèse des vertébrés. Arch Biol 55: 1–286

Erickson CA, Loring JF, Lester SM (1989) Migratory pathways of HNK-1-immunoreactive neural crest cells in the rat embryo. Dev Biol 134: 112–118

Fritzsch B, Northcutt RG (1993) Cranial and spinal nerve organization in amphioxus and lampreys: evidence for an ancestral craniate pattern. Acta Anat 148: 96–109

Gould SJ (1977) Ontogeny and Phylogeny. Harvard University Press, Cambridge, Mass

Hall BK, Hörstadius S (1988) The Neural Crest. Oxford Science Publications, London

Hardisty MW (1981) The skeleton. In "The Biology of Lampreys 3" Ed by MW Hardisty, IC Potter, Academic Press, London, pp 333–376

Healey EG (1972) The central nervous system. In "The Biology of Lampreys 2" Ed by MW Hardisty, IC Potter, Academic Press, London, pp 307–372

Hirata M, Ito K, Tsuneki K (1997) Migration and colonization patterns of HNK-1-immunoreactive neural crest cells in lamprey and swordtail embryos. Zool Sci 14: 305–312

Hou L, Takeuchi T (1994) Neural crest development in reptilian embryos, studied with monoclonal antibody, HNK-1. Zool Sci 11: 423–431

Johnston JB (1908) Additional notes on the cranial nerves of petromyzonts. J Comp Neurol Psychol 18: 569–608

Kuratani S, Ueki T, Aizawa S, Hirano S (1997) Peripheral development of cranial nerves in a cyclostome, *Lampetra japonica*: morphological distribution of nerve branches and the vertebrate body plan. J Comp Neurol 384: 483–500

Langille RM, Hall BK (1988) Role of the neural crest in development of the trabeculae and branchial arches in embryonic sea lamprey, *Petromyzon marinus* (L). Development 102: 301–310

Laudel TP, Lim T-M (1993) Development of the dorsal root ganglion in a teleost, *Oreochromis mossambicus* (Peters). J Comp Neurol 327: 141–150

Le Douarin NM (1982) The Neural Crest. Cambridge University Press, Cambridge

Loring JF, Erickson CA (1987) Neural crest cell migratory pathways in the trunk of the chick embryo. Dev Biol 121: 220–236

McKinney ML, McNamara KJ (1991) Heterochrony: The Evolution of Ontogeny. Plenum Press, New York

Morin-Kensicki EM, Eisen JS (1997) Sclerotome development and peripheral nervous system segmentation in embryonic zebrafish. Development 124: 159–167

Newth DR (1956) On the neural crest of the lamprey embryo. J Embryol Exp Morph 4: 358–375

Nicol JAC (1952) Autonomic nervous systems in lower chordates. Biol Rev 27: 1–49

Nishikawa S, Sasaki F (1993) Secretion of chondroitin sulfate from embryonic epidermal cells in *Xenopus laevis*. J Histochem Cytochem 41: 1373–1381

Reissmann E, Ernsberger U, Francis-West PH, Rueger D, Brickell PM, Rohrer H (1996) Involvement of bone morphogenetic protein-4 and bone morphogenetic protein-7 in the differentiation of the adrenergic phenotype in developing sympathetic neurons. Development 122: 2079–2088

Richardson MK (1995) Heterochrony and the phylotypic period. Dev Biol 172: 412–421

Sadaghiani B, Vielkind JR (1989) Neural crest development in *Xiphophorus* fishes: scanning electron and light microscopic studies. Development 105: 487–504

Sadaghiani B, Vielkind JR (1990) Distribution and migration pathways of HNK-1-immunoreactive neural crest cells in teleost fish embryos. Development 110: 197–209

Sadaghiani B, Crawford BJ, Vielkind JR (1994) Changes in the distribution of extracellular matrix components during neural crest development in *Xiphophorus* spp. embryos. Can J Zool 72: 1340–1353

Shah NM, Groves AK, Anderson DJ (1996) Alternative neural crest cell fates are instructively promoted by TGFβ superfamily members. Cell 85: 331–343

Tahara Y (1988) Normal stages of development in the lamprey, *Lampetra reissneri* (Dybowski). Zool Sci 5: 109–118

Tavolga WN (1949) Embryonic development of the platyfish (*Platypoecilus*), and the swordtail (*Xiphophorus*) and their hybrids. Bull Amer Mus Nat Hist 94: 165–229

Teillet MA, Kalcheim C, Le Douarin NM (1987) Formation of the dorsal root ganglia in the avian embryo: segmental origin and migratory behavior of neural crest progenitor cells. Dev Biol 120: 329–347

Wright GM (1986) Immunocytochemical study of fibronectin in the sea lamprey, *Petromyzon marinus*, and the Atlantic hagfish, *Myxine glutinosa*. Cell Tissue Res 244: 549–555